

## Low temperature hydrothermal synthesis of calcium phosphate ceramics: Effect of excess Ca precursor on phase behaviour

Asep Sofwan Faturohman Alqap<sup>a, b</sup> & Iis Sopyan<sup>a, \*</sup>

<sup>a</sup>Department of Manufacturing and Materials Engineering, Faculty of Engineering, International Islamic University Malaysia (IIUM), P O Box 10, Kuala Lumpur 50728, Malaysia

<sup>b</sup>Mechanical Engineering Program, Faculty of Engineering, University of Bengkulu, Jalan Raya Kandang Limun, Bengkulu 38000, Indonesia  
Email: sopyan@iiu.edu.my

*Received 31 July 2009; revised and accepted 20 October 2009*

Low temperature hydrothermal exchange reaction has been used to synthesize calcium phosphate materials comprising hydroxyapatite and  $\beta$ -tricalcium phosphate using CaO and  $\text{NH}_4\text{H}_2\text{PO}_4$  as calcium and phosphorus precursors respectively. The effect of excess of calcium precursor on phase behaviour of these materials has been investigated by varying CaO content (0, 10 and 20 mole% excess of 0.1 mole CaO) in the suspension. The as-synthesized paste has been dried followed by calcination at 700-1200 °C. Results show the formation of Ca-deficient apatite at the lower calcination temperature. Excess of CaO shifts the balance to hydroxyapatite formation at the higher calcination temperature such that  $\beta$ -tricalcium phosphate,  $\beta$ -tricalcium phosphate + hydroxyapatite and hydroxyapatite of higher purity are obtained with 0, 10 and 20 mole% excess CaO, respectively.

**Keywords:** Hydrothermal synthesis, Hydroxyapatites, Calcium deficient apatites, Calcination, Ceramics, Calcium phosphates

**IPC Code:** Int. Cl.<sup>9</sup> C04B35/447

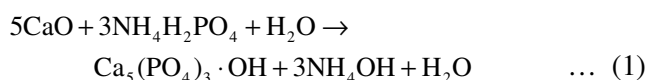
Calcium phosphate has been studied as bone repair materials for the last 80 years<sup>1</sup>. The use of calcium phosphate biomaterials, particularly hydroxyapatite (HA) and tricalcium phosphate (TCP), has gained popularity due to their excellent biocompatibility, bioactivity and osteoconductivity attributed to the close chemical resemblance with the mineral component of natural bone and teeth<sup>2,3</sup>. HA and TCP have been used, not only for bone implant substitute materials<sup>1,2</sup>, but have also been identified for applicability as drug delivery<sup>4</sup>, antiseptics<sup>5</sup>, food supplements<sup>6</sup>, and hyperthermia treatment agents<sup>7,8</sup>. The potential of the material as anticancer agent has been investigated and it has been found that nanoscale HA is effective in inhibiting cancer cells growth<sup>9,10</sup>.

The success of calcium phosphate-based biomaterials in biomedical application depends largely on the availability of highly pure, crystalline HA with fine particle size, enabling improved biological and mechanical properties. Intensive studies on calcium phosphate involving a wide range of powder processing techniques have been carried out with the aim of producing HA powder with well defined particle morphology<sup>11</sup>. Numerous synthesis techniques have been developed to produce HA such as solid state reaction, microwave processing, pH shockwave, hydro-

thermal and wet precipitation. Differences in the preparative routes lead to variations in morphology, stoichiometry, and level of crystallinity. Amongst these methods, the most commonly used technique is the precipitation technique involving wet chemical reactions between calcium and phosphorus precursors under controlled temperature and pH conditions. Other methods such as sol-gel, spray pyrolysis and mechano-chemical method, have also been developed and well documented<sup>12,13</sup>. The advantage of the wet precipitation technique which involves aqueous solution is that its by-product is mostly water and the probability of contamination during processing is very low<sup>11</sup>. However, a long ageing time is required to allow the precipitation reaction to end, as keeping the single ion concentration uniform during the precipitation stage is very difficult<sup>14</sup>. Although many studies on apatite based calcium phosphate by wet precipitation technique have been reported, the use of calcium oxide as calcium precursor is rather scarce. In the present study, calcium oxide was reacted with ammonium di-hydrogen phosphate to yield HA through a low temperature hydrothermal exchange reaction. Investigation on the effect of excess calcium precursor on the phase behaviour of the calcium phosphate is also presented.

## Materials and Methods

The apatite based calcium phosphate was prepared using calcium oxide granules (CaO) (Techno Pharmchem, India) and ammonium di-hydrogen phosphate ( $\text{NH}_4\text{H}_2\text{PO}_4$ ) (System, Malaysia) as the precursors with distilled water as the solvent. For the preparation of the solution, stoichiometric weight of 0.1 mole calcium oxide was mixed in 100 ml distilled water with vigorous stirring to get a soluble suspension. Into this suspension, ammonium dihydrogen phosphate powder on the base of 1.67 Ca/P was then added dropwise such that the fluidity of the suspension remained constant. The suspension was heated until its temperature reached 90 °C when a paste was obtained. The overall process may be represented as in Eq.(1).



The paste was dried overnight at 80 °C in a drying oven before the next characterization. Three samples were synthesized: **Ca-0** for no CaO excess, **Ca-1** for 10 mole% excess CaO and **Ca-2** for 20 mole% excess CaO added to 0.1 mole CaO as the stoichiometric basis. The prepared powders were then calcined in a Protherm PLF 160/5 furnace at 700-1200 °C. A heating rate of 10 °C min<sup>-1</sup> was applied until the required temperature was reached and then the heating was continued for 1 hour.

To identify the functional groups of the samples, Fourier transform infrared (FTIR) spectra were recorded using a Perkin-Elmer Spectrum 100 FTIR spectrometer over 4000-400 cm<sup>-1</sup> with scanning range at a 4 cm<sup>-1</sup> resolution. Using CuK $\alpha$  radiation ( $\lambda = 1.5406$  nm), X-ray diffraction pattern were obtained on a Shimadzu XRD 6000 diffractometer. Scan speed of 2° per minute and a step size of 0.02° over the 2 $\theta$  range of 20-50° were used. Crystallographic identification of the phases of synthesized apatite was done by comparing the experimental XRD patterns to standards of the Joint Committee on Powder Diffraction Standards (JCPDS) card number 09-0432, Markovic *et al.*'s published data for HA<sup>15</sup>, JCPDS 09-169 whitlockite mineral and Ernrich & Peters published data for  $\beta$ -tricalcium phosphate<sup>16</sup>. The as-synthesized powders were subjected to thermal analysis using a heating rate of 2 °C min<sup>-1</sup> over 30-1150 °C in air atmosphere using a Perkin-Elmer Phyris Diamond TG-DTA instrument.

## Results and Discussion

### FTIR spectra

To study the evolution of functional groups in the samples calcined at different temperatures, the FTIR spectra of the samples were analysed. The functional groups normally observed in the FTIR of calcium phosphate based materials are  $\text{PO}_4^{3-}$ ,  $\text{OH}^-$ ,  $\text{HPO}_4^{2-}$  and  $\text{CO}_3^{2-}$  in the range of 4000-300 cm<sup>-1</sup>. The  $\text{PO}_4$  bands appear at around 1100-1019 cm<sup>-1</sup> for  $\nu_3$  mode, 958 cm<sup>-1</sup> for  $\nu_1$  mode, 605-530 cm<sup>-1</sup> for  $\nu_4$  mode and 500-400 cm<sup>-1</sup> for  $\nu_2$  mode. There are three modes of  $\text{OH}^-$  ions, i.e., stretching, vibrational, and translational modes at 3700-2500, 630 and 390 cm<sup>-1</sup>, respectively<sup>15</sup>. The  $\text{HPO}_4^{2-}$  ions are observed at 875 cm<sup>-1</sup> band. Overtone and combination of the  $\nu_3$  and  $\nu_1$   $\text{PO}_4$  modes or even  $\text{HPO}_4^{2-}$  appear in the 2200-1950 cm<sup>-1</sup> region<sup>15,17</sup>. Water molecules appear at 1642 cm<sup>-1</sup> but may be obscured by the  $\text{CO}_3$  band<sup>17,18</sup>. The  $\nu_1$  band of  $\text{CO}_3$  may be superimposed with bands of  $\text{HPO}_4^{2-}$  and  $\nu_3$   $\text{PO}_4$  at 1089 cm<sup>-1</sup> (refs 17,19). The  $\text{CO}_3^{2-}$  ions, which replace  $\text{PO}_4^{3-}$  ions in the HA lattice (designated as the "B-type" carbonate) appear at about 1410 and 1450 cm<sup>-1</sup>. Appearance of bands at 1210, 1188 and 1115 cm<sup>-1</sup> where  $\text{CO}_3^{2-}$  possibly replaces  $\text{PO}_4^{3-}$  ion, strengthens the identity of the "B-type" carbonate<sup>17</sup>.  $\text{CO}_3^{2-}$  that are supposed to replace  $\text{OH}^-$  ions in the HA lattice (designated as the "A-type" carbonate), if any, are at 1455 cm<sup>-1</sup> and 1540 cm<sup>-1</sup> (ref. 20).

Figure 1 shows the representative FTIR spectra for the sample **Ca-0**, calcined at 700, 900, and 1200 °C. The sample **Ca-0** calcined at 700°C show bands at 1089 cm<sup>-1</sup> of  $\text{HPO}_4^{2-}$  or  $\text{PO}_4^{3-}$  ( $\nu_3$ ), at 1020 of  $\text{PO}_4$  ( $\nu_3$ ), at 958 of  $\text{PO}_4$  ( $\nu_1$ ), at 875 of  $\text{HPO}_4^{2-}$ , at 630 of  $\text{OH}^-$  (librational), and at 600 and 560 of  $\text{PO}_4$  ( $\nu_4$ ). These bands indicate that the sample contains  $\text{HPO}_4$ ,  $\text{PO}_4$ , and  $\text{OH}^-$ , suggesting the formation of calcium deficient HA (CDHA) with the formula  $\text{Ca}_9(\text{HPO}_4)(\text{PO}_4)_5\text{OH}$ . The bands at higher wave number range also appear with weak intensities. These are at 3700-2600 of  $\text{OH}^-$  (stretching), at 1643 of water molecules or  $\text{CO}_3$ , and at 1442-1419 of  $\text{CO}_3$ .

No change in position is observed for the bands at 1089, 1020, and 600 cm<sup>-1</sup> over the calcination range of 700-1200°C. Along with the band at 958 cm<sup>-1</sup>  $\text{PO}_4$  ( $\nu_1$ ) observed in the sample calcined at 700°C, in sample calcined at 800°C, two new bands at 970 and 945 cm<sup>-1</sup>; these are observed in samples calcined up to 1200°C. The band at 875 cm<sup>-1</sup> for  $\text{HPO}_4$  and at 630 cm<sup>-1</sup> for  $\text{OH}^-$  disappear in the sample calcined at

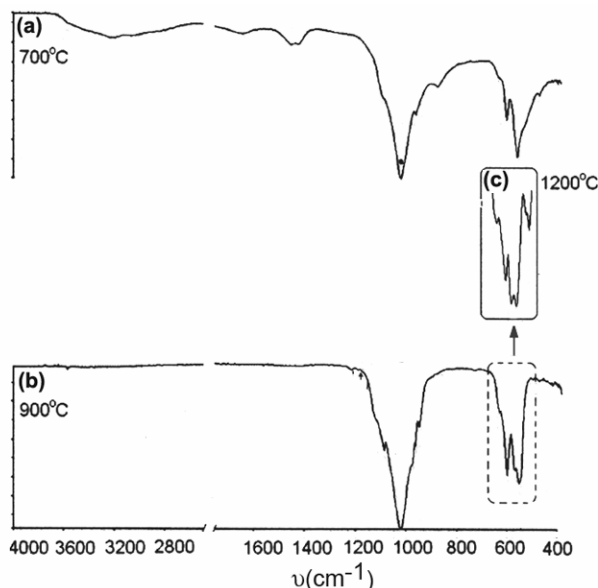


Fig. 1 – The IR spectra of sample **Ca-0** calcined at (a) 700°C; (b) 900°C and (c) 1200°C.

800°C and instead, the band for  $P_2O_7$  appears at  $727\text{ cm}^{-1}$ ; the band intensity tends to increase up to 1200°C. The  $PO_4$  band at  $600\text{ cm}^{-1}$  appears at 700°C with the band at  $589\text{ cm}^{-1}$  appears weaker at the higher temperature. The band at  $559\text{ cm}^{-1}$   $PO_4$  ( $\nu_4$ ) appears at 700°C with two new bands seen at 545 and  $495\text{ cm}^{-1}$  at 800°C. The  $495\text{ cm}^{-1}$  band still appears up to 1200°C, but the 545 band splits into two, to give bands at 550 and  $536\text{ cm}^{-1}$  at 1200°C. The disappearing or reducing bands due to  $HPO_4$  and OH along with appearance of band due to  $P_2O_7$  and two new bands of  $PO_4$  at 970 and  $945\text{ cm}^{-1}$  show the appearance of TCP in the samples as also confirmed by the X-ray data. It is noteworthy that non-single peak between 1019-900 and/or more than two peaks in the range  $600\text{-}500\text{ cm}^{-1}$  are indicators of the non-HA phase.

On heating at  $\geq 800^\circ\text{C}$ , the bands at  $630\text{ cm}^{-1}$  due to OH and at  $875\text{ cm}^{-1}$  due to  $HPO_4$  disappear, and band due to  $P_2O_7$  at  $727\text{ cm}^{-1}$  arises. The band at  $875\text{ cm}^{-1}$  is possibly due to replacement of  $PO_4$  by  $CO_3$  as suggested by Santos & Clayton<sup>20</sup>. Besides the  $958\text{ cm}^{-1}$  peak, two other peaks at 970 and  $945\text{ cm}^{-1}$  appear. The presence of these two peaks along with the  $727\text{ cm}^{-1}$  peak indicates that the phase is  $\beta$ -TCP, and not HA, as indicated from the X-ray patterns (shown later in Fig. 2). Moreover, not only is the  $727\text{ cm}^{-1}$  band observed but also seen are the bands at 1165 and  $1124\text{ cm}^{-1}$  due to  $P_2O_7$  (ref. 21). With increasing temperature, the unreacted phosphorus monomer may be

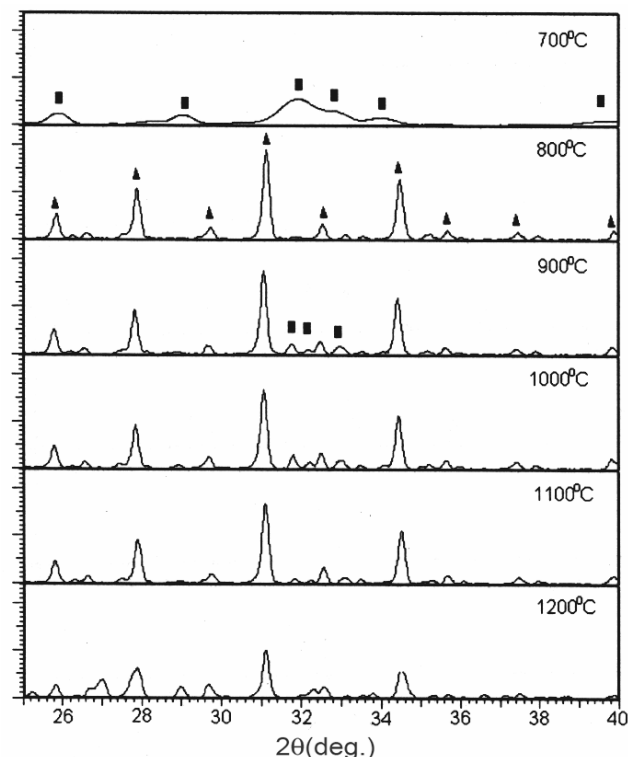


Fig. 2 – X-ray spectra of the sample **Ca-0** calcined at temperatures of 700 -1200°C. [■ HA; ▲ TCP].

oxidized to  $HPO_4$ , which then condenses to produce  $P_2O_7$  and  $H_2O$  at higher temperatures.

The spectra of the sample **Ca-1** calcined at 700°C show the same peak positions as of the sample **Ca-0**, i.e., bands at 1089, 1019, 958, 875, 630, 600, and  $559\text{ cm}^{-1}$ . However, there are changes in the spectra of samples calcined at 800-1200°C. The  $630\text{ cm}^{-1}$  OH<sup>-</sup> band increases in resolution up to 1000°C and then decreases for the higher temperatures suggesting an increase and decrease in HA respectively. After 800°C, the  $559\text{ cm}^{-1}$   $PO_4$  ( $\nu_4$ ) blunts and other peaks arise between 530 and  $570\text{ cm}^{-1}$  as was observed for sample **Ca-0**. The  $P_2O_7$  band at  $727\text{ cm}^{-1}$  appears after 800°C and becomes stronger up to 1100°C, but disappears again at 1200°C. After 800°C, some new peaks arise before and after the  $958\text{ cm}^{-1}$   $PO_4$  ( $\nu_1$ ) band which becomes stronger up to 1100°C, but is significantly reduced at 1200°C. All these suggest the appearance of non-HA phase. The increase in number of peaks is also been in the range of  $1200\text{-}1020\text{ cm}^{-1}$  along with increase in the  $P_2O_7$  peak at  $727\text{ cm}^{-1}$ . The functional group characteristics of the sample **Ca-1** are not generally different from those of sample **Ca-0**, except that the latter has no OH (librational) in its spectra after calcination at 800°C.

The increase in the  $630\text{ cm}^{-1}$  OH band until  $1000^\circ\text{C}$  and decrease above  $1000^\circ\text{C}$ , accompanied by the appearance of  $727\text{ cm}^{-1}$   $\text{P}_2\text{O}_7$  band which decreases at  $1200^\circ\text{C}$ , and also the appearance of  $\text{PO}_4$  peaks at  $970$  and  $945\text{ cm}^{-1}$  are all indicators of the biphasic CaP, i.e., containing both HA and  $\beta$ -TCP. Therefore, it is concluded that the  $970$  and  $945\text{ cm}^{-1}$  bands may be attributed to  $\beta$ -TCP. This is also supported by the fact that a decrease in resolution of the two peaks at  $975$  and  $940\text{ cm}^{-1}$  was observed at  $1200^\circ\text{C}$ , indicating that the appearance of  $\beta$ -TCP is likely during the conversion process to another phase, which is most probably  $\alpha$ -TCP.

In the IR spectra of the sample **Ca-2** calcined at  $700$ - $1200^\circ\text{C}$ , the upper region, i.e.,  $4000$ - $1300\text{ cm}^{-1}$ , shows the bands as observed in the samples **Ca-0** and **Ca-1** after calcination at  $700^\circ\text{C}$ ; these disappear after calcination at  $800^\circ\text{C}$  and above. The characteristic peaks of **Ca-2**, in the region of  $1250$ - $400\text{ cm}^{-1}$ , are also the same as those of the samples **Ca-0** and **Ca-1** after calcination at  $700^\circ\text{C}$ . The  $1020\text{ cm}^{-1}$  band of  $\text{PO}_4$  ( $\nu_3$ ) and  $559\text{ cm}^{-1}$  band of  $\text{PO}_4$  ( $\nu_4$ ) show the highest transmittance. These are accompanied by bands at  $1089\text{ cm}^{-1}$  of  $\text{PO}_4$  ( $\nu_3$ ),  $958\text{ cm}^{-1}$  of  $\text{PO}_4$  ( $\nu_1$ ),  $875\text{ cm}^{-1}$  of  $\text{HPO}_4$ ,  $630\text{ cm}^{-1}$  of OH (librational) and  $600\text{ cm}^{-1}$  of  $\text{PO}_4$  ( $\nu_4$ ). However, the companion peaks as HA characteristic peaks as mentioned earlier increase in transmittance with the increase in calcination temperatures and are stable up to  $1100^\circ\text{C}$ . The transmittance of these peaks reduces after calcination at  $1200^\circ\text{C}$ , indicating a change in phase. The characteristic peaks differentiate the sample **Ca-2** from the other two samples, **Ca-0** and **Ca-1**. Here it is likely that HA exists as a single and stable phase at all calcination temperatures, unless the X-ray data indicates  $\beta$ -TCP as trace.

The **Ca-2** sample has a distinct IR pattern, and the main peaks are stable at all the calcination temperatures. Particularly, the  $\text{PO}_4$  ( $\nu_1$ ) remains as a single peak at  $958\text{ cm}^{-1}$  and the  $\text{PO}_4$  ( $\nu_4$ ) at  $559\text{ cm}^{-1}$  is also stable. It is also interesting to note that the existence of the  $\text{CO}_3$  and  $\text{HPO}_4$  bands in the range of  $3800$ - $1400\text{ cm}^{-1}$  do not affect the stability of the bands at  $1089$ ,  $1019$ ,  $958$ ,  $600$  and  $559\text{ cm}^{-1}$  of  $\text{PO}_4$  and at  $630\text{ cm}^{-1}$  for OH, which was not been in the spectra of the **Ca-0** and **Ca-1** samples. All these six bands are characteristics for HA as confirmed by the X-ray data. Thus, the sample **Ca-2** has the IR spectra of the HA phase pattern at all the higher temperatures. An increase in the amount of HA is also observed here, as observed by

the increase in intensity of the OH (librational) band in particular, and the characteristic companion peaks in general, with temperature. Even though P-OH or  $\text{HPO}_4$  bands are observed, the excess calcium prevents the condensation reaction of  $\text{HPO}_4$  to  $\text{P}_2\text{O}_7$  and water. As a result, the transformation from CDHA to  $\beta$ -TCP is not observed in the **Ca-2** sample.

While the three samples after calcination at  $700^\circ\text{C}$  have the same spectra in general, but in more detail, the samples show a small difference in the region of  $559$ - $466\text{ cm}^{-1}$ . Other  $\text{PO}_4$  peaks, i.e.  $\nu_4$  or  $\nu_1$  mode, tend to show up. Hence, an adjustment of band position between  $545$  and  $559\text{ cm}^{-1}$  of the highest peak in transmittance of  $\text{PO}_4$  ( $\nu_4$ ) which is observed in the samples **Ca-0** and **Ca-1** at all heating temperatures is not seen in sample **Ca-2**. This suggests that the appearance of  $\text{PO}_4$  ( $\nu_4$ ) peak position has been affected by calcium. After  $800^\circ\text{C}$ , P-OH or  $\text{HPO}_4$  which is observed in sample **Ca-0** condenses to form  $\text{P}_2\text{O}_7$  and  $\text{H}_2\text{O}$  immediately at this temperature or even at lower calcination temperatures but with longer dwell time as suggested by Markovic *et al.*<sup>15</sup> Once  $\text{P}_2\text{O}_7$  appears and OH disappears, the sample will have no more HA.

The presence of  $\text{H}_2\text{O}$  as the by-product of the  $\text{HPO}_4$  condensation reaction, or from water bonded to some intermediates, or even from the atmosphere is likely to affect the number of hydroxyl ions in the apatite crystal. However, as the hydroxyl ions in HA crystal occupies a site slightly above or below the triangular calcium plane, the replacement of hydroxyl, by carbonate for example, does not significantly affect the overall crystal system. A significant change will take place if carbonate is replaced by phosphate, leading to change in the  $a$ -lattice parameter<sup>22</sup>. Thus, the presence of carbonate ions affects the order within the apatite structure. This is thought to yield disordered arrangement of phosphate ions that do not assemble in the expected hexagonal structure defining an ideal HA crystal system.

#### X-ray analysis

Figure 2 shows the X-ray patterns of the sample **Ca-0** calcined at  $700$ - $1200^\circ\text{C}$ . It shows the  $700^\circ\text{C}$ -calcined sample is totally different from those calcined at higher temperatures. The X-ray pattern indicates that the  $700^\circ\text{C}$  sample characterizes HA peaks of low crystallinity, while at  $800^\circ\text{C}$ , the  $\beta$ -TCP peaks appear as the main phase. At  $900^\circ\text{C}$  and above, HA appears again with very weak intensity. The X-ray pattern of  $1200^\circ\text{C}$  calcined sample suggests that the  $\beta$ -TCP is no longer stable in the sample **Ca-0** as

its intensity decreases. It is likely to be transformed to  $\alpha$ -TCP. However, no  $\alpha$ -TCP identified in the pattern indicates that the transformation is just beginning. One study has reported that the transformation to  $\alpha$ -TCP starts at 1160°C (ref. 17).

Table 1 shows the main peaks within the range of 25–40° in  $2\theta$  for all the samples after calcination at 700°C and for comparison, data of HA according to JCPDS 09-0432. Table 1 suggests that one of the HA peaks, i.e., (112), of the sample **Ca-0** is unresolved because the peak is too broad. In addition, the  $2\theta$  positions shift to the left or to the right of the standard HA positions. This suggests the appearance of calcium-deficient hydroxyapatite. The fraction of crystalline phase ( $X_c$ ) in the HA powders can be evaluated by Eq.(2) (ref. 23),

$$X_c = 1 - V_{(112)/(300)} / I_{(300)} \quad \dots (2)$$

where  $V_{(112)/(300)}$  is the intensity of the hollow between (112) and (300) diffraction peaks of HA and  $I_{(300)}$  is the intensity of (300) diffraction peak. The fraction of HA crystalline phase ( $X_c$ ) of the sample **Ca-0** calcined at 700°C is only 0.205, and HA does not exist at higher calcinations temperatures (Fig. 2). The lattice parameters of the three samples have been compared with those previously reported for HA and  $\beta$ -TCP (henceforth referred to as the standard)<sup>15,16</sup>. The lattice parameter of the sample **Ca-0** for HA phase at 700°C (9.433 Å) is higher than standard  $a$ -lattice (9.418 Å), but less than the  $c$ -lattice. Regarding HA phase atomic spacing ( $d$ ), the values at around  $2\theta = 25.86$  and  $34.04^\circ$  of the sample **Ca-0**, i.e., 3.436 and 2.629 Å respectively, are lower than those of the standard values i.e., 3.440 and 2.630 Å. When the calcination temperature increases to 800°C, the sample **Ca-0** has  $\beta$ -TCP as the single phase. The X-ray patterns indicate no identifiable change in peak with increasing temperature, except at 1200°C calcination where enrichment in peak number was observed indicating the instability of the phase. At  $\geq 800^\circ\text{C}$  where  $\beta$ -TCP is the main phase of the sample **Ca-0**,

the  $a$ -lattice parameters of the sample for 800, 900, 1000, 1100 and 1200°C are 10.446, 10.429, 10.429, 10.468 and 10.429 Å respectively with an average of 10.440 Å; while for the  $c$ -lattices parameter these values are 37.375, 37.380, 37.380, 37.282 and 37.380 Å respectively with an average of 37.359 Å. These average values are in good agreement with their standard values 10.429 and 37.380 Å, respectively. The parameter  $d$  of the sample **Ca-0** arbitrarily taken at  $2\theta = 25.782$  and  $34.398^\circ$  gave the average values of 3.461 and 2.601 Å, which are very close to the standard values, 3.453 and 2.605 Å, respectively.

Figure 3 shows the X-ray patterns of the sample **Ca-1** calcined at 700–1200°C. It is observed that HA or calcium-deficient apatite peaks appear as a broad pattern such that the (112) peak is unresolved (see Table 1). The fraction of crystalline phase ( $X_c$ ) is

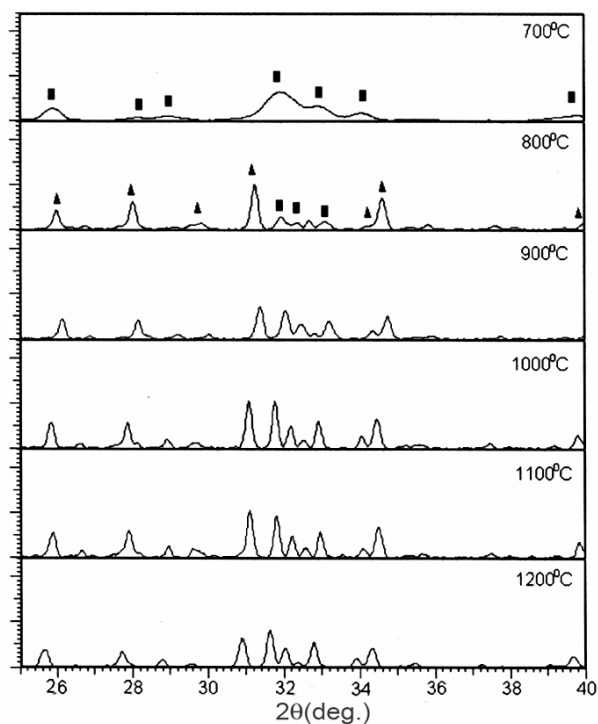


Fig. 3 – X-ray spectra of the sample **Ca-1** calcined at temperatures of 700–1200°C. [■ HA; ▲ TCP].

Table 1 – The positions of main peaks of all the samples after calcination at 700°C

	2θ (deg.)							
	(002)	(102)	(210)	(211)	(112)	(300)	(202)	(310)
HA <sup>a</sup>	25.879	28.126	28.966	31.773	32.196	32.902	34.048	39.818
<b>Ca-0</b>	25.885	28.28	29.012	31.88	n.a.	32.64	34	39.65
<b>Ca-1</b>	25.869	28.2	28.925	31.957	n.a.	32.9	34.01	39.66
<b>Ca-2</b>	25.87	28.14	29.17	32.04	n.a.	32.88	34.035	39.595

<sup>a</sup>According to JCPDS # 09-0432.

0.259. As the IR spectra show, the OH (librational) band is clearly observed at higher calcination temperatures at 800-1200°C, leading to identifiable HA peaks in the X-ray spectra. The intensities of the HA peaks also increase with increase in temperature. The fractions of crystalline phase ( $X_c$ ) of the HA for 800, 900, 1000, 1100 and 1200°C are 0.443, 0.689, 0.786, 0.820 and 0.799 respectively. It is clear that a significant improvement in the crystalline fraction does not occur after 1000°C. Figure 3 also indicates that  $\beta$ -TCP is the main phase at 800°C and above. The  $\beta$ -TCP intensities do not increase significantly from 800°C (500 cps) to 1100°C (520 cps), and decrease significantly at 1200°C (350 cps), although the indication for  $\beta$ -TCP getting transformed to  $\alpha$ -TCP has not yet appeared. The average value of the  $a$ - and  $c$ -lattice parameters over 800-1200°C (i.e., 9.422 and 6.895 Å respectively) are closer to the standard values for HA phase (i.e., 9.418 and 6.884 Å respectively) and identical to the standard for values TCP phase (i.e., 10.429 and 37.380 Å respectively). There is no disruption of the lattice parameters in TCP. The  $a$ - or  $c$ -lattice parameter of HA tends to fluctuate for different temperatures although an increasing trend is also observed. For TCP, however, the value of parameters is constant over the range of 800-1200°C.

The X-ray patterns of the sample **Ca-2** calcined at 700-1200°C (Fig. 4) show that the HA (112) is unresolved at 700°C (see Table 1) indicating the calcium-deficient hydroxyapatite phase. When calcined at 800°C, the HA peaks appear as four peaks in the range of  $2\theta = 31.77$ - $34.05^\circ$ , i.e., (211), (112), (300), and (202). The fraction of HA crystalline phase ( $X_c$ ) increases with increase in temperature, i.e., 0.257, 0.651, 0.795, 0.889, 0.935 and 0.961 at 700, 800, 900, 1000, 1100 and 1200°C respectively. This quantitatively proves that significant improvement in the fraction of crystallinity can be obtained by elevating the calcination temperature. The  $\beta$ -TCP is still invisible at 700°C and appears when the sample is calcined at 800°C but decreases in intensity with the increased temperatures (Fig. 4). In the 1200°C-calcined sample, even the  $\beta$ -TCP peak is insignificant. The single P-O band of  $958\text{ cm}^{-1}$  (for  $\nu_1\text{ PO}_4$ ) and two P-O bands of  $600\text{ cm}^{-1}$  and  $559\text{ cm}^{-1}$  (both for  $\nu_4\text{ PO}_4$ ) as well as  $630\text{ cm}^{-1}$  band for OH (librational), are characteristic peaks for HA.

The HA phase of the sample **Ca-2** is the main phase of the sample. The average values of the  $a$ - and  $c$ - lattice parameters of **Ca-2** over 700-1200°C

(i.e., 9.401 and 6.874 Å respectively) are lower than those of the HA standard (i.e., 9.418 and 6.884 Å respectively). The  $a$ - and  $c$ -lattice parameters change with the CaO content. For the  $a$ - and  $c$ - lattice parameters, it is observed that  $a_{\text{Ca-0}} > a_{\text{Ca-1}} = a_{\text{TCP}}$  and  $c_{\text{Ca-0}} < c_{\text{Ca-1}} = c_{\text{TCP}}$  for TCP phase;  $a_{\text{Ca-1}} \approx a_{\text{HA}} > a_{\text{Ca-2}}$  and  $c_{\text{Ca-1}} > c_{\text{HA}} > c_{\text{Ca-2}}$  for HA phase, while the average values of atomic spacing shows the trend:  $d_{\text{Ca-0}} = d_{\text{Ca-1}} > d_{\text{TCP}}$  for TCP and  $d_{\text{Ca-1}} > d_{\text{HA}} \approx d_{\text{Ca-2}}$  for HA. One reason for this trend in  $d$  is that impurities (such as carbonate), play a role in influencing the crystal system of the samples. Santos and Clayton<sup>20</sup> have reported that carbonate substitution has a negative correlation with the  $a$ -lattice parameter. The value of parameters here fluctuates suggesting that variation in carbonate has occurred due to uncontrolled atmosphere. There may be another possible reason, i.e., the secondary phase which has been observed may affect the crystal system. The contraction in the  $a$ -parameter is likely to be compensated by the expansion in the  $c$ -parameter, and vice versa, such that the ratio,  $c/a$ , is kept the same and, as a result, the atomic spacing of the samples is closer to that of the standard.

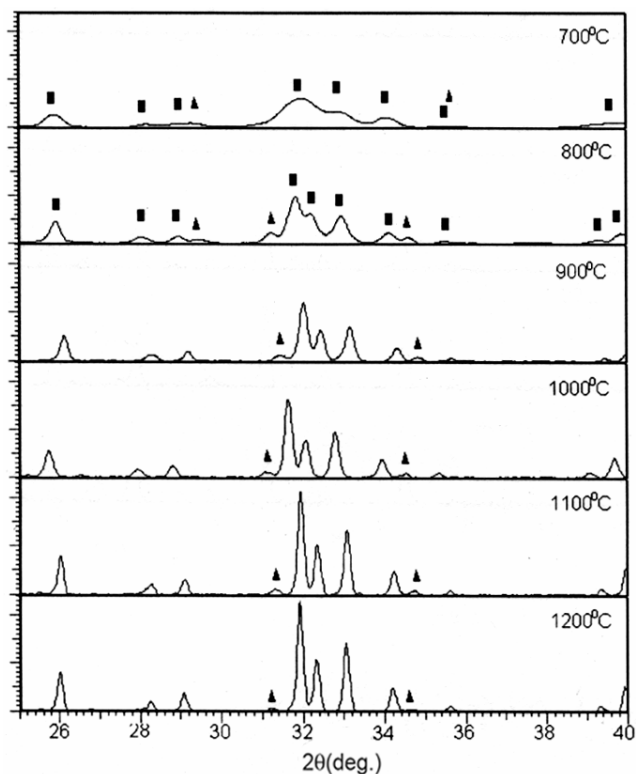
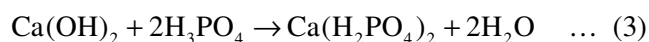


Fig. 4 – X-ray spectra of the sample **Ca-2** calcined at temperatures of 700 -1200°C. [■ HA; ▲ TCP].

We have also carried out studies on 1 and 2 mole% excess of CaO with 0.125 mole CaO as the basis (7 g CaO and 8.63 g  $\text{NH}_4\text{H}_2\text{PO}_4$ ) in 150 ml distilled water. The principal difference between 1 and 10 mole% excess CaO samples is that the former, i.e., 1 mole% excess has no HA and only  $\beta$ -TCP at all calcination temperatures employed where the  $\beta$ -TCP shows around 600 cps of the main peak intensity (0210) for 900°C calcination temperature. The latter, i.e., 10 mole% excess, has  $\beta$ -TCP and HA with the main peak intensity of  $\beta$ -TCP around 370 cps. There is no difference in the phase appearance between the 2 and 20 mole% excess CaO samples. Both give HA as main phase with  $\beta$ -TCP as traces, however, the 2 mole% excess sample has the HA main peak (211) intensity of around 850 cps, higher than that of 20 mole% excess around 600 cps for 900°C calcination temperature.

Thermogravimetry analysis of the samples **Ca-0**, **Ca-1**, and **Ca-2** give information regarding the influence of excess CaO on reaction commencement as observed from weight loss. The phase transformations generally require heat as DT analyses indicate, except in the final stages when heat is released and the corresponding phase possibly begins transforming to further phase at higher temperature. The weight losses detected are mainly due to a decrease in amount of O-H groups of intermediate phase reaction. The common pattern in the TG curves of the three samples reveals four reaction sites in the ranges of 40-100°C, 100-250°C, 250-600°C and 600-800°C. These may be attributed to the loss of residual water for the first, water and ammonia evaporations for the second and the third, and densification and crystallization for the fourth range. The TG curves show the difference in weight losses until ~700°C, with the sample **Ca-0** showing the lowest and **Ca-2** the highest loss. At around 700°C, it is seen that the temperature at which the weight loss occurs decreases and weight loss level increases with the increase in excess calcium. It has been reported earlier that the weight losses at ~700°C is probably due to removal of water as the by-product from the reaction of  $\text{P}_2\text{O}_7^{4-}$  ions with lattice  $\text{OH}^-$  ions, forming TCP<sup>24</sup>. However, this is not true in this study since the sample **Ca-0**, with the highest portion of TCP, showed the least weight loss. It is suggested that the loss is due to deviation from the stoichiometric reaction as the reaction using excess Ca precursor removes more reactants.

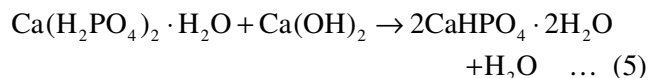
It is noteworthy that the TG curves of the samples **Ca-0** and **Ca-1** show multiple losses, compared to the single weight loss for sample **Ca-2**. The multiple losses in the TG pattern are probably due to multiple reactions. It is proposed that calcium hydroxide appears from the reaction of CaO with water and, phosphoric acid ( $\text{H}_3\text{PO}_4$ ) and ammonium hydroxide ( $\text{NH}_4\text{OH}$ ) from hydrolysis of ammonium dihydrogen phosphate ( $\text{NH}_4\text{H}_2\text{PO}_4$ ). The reaction of calcium hydroxide and phosphoric acid will then produce calcium dihydrogen phosphate ( $\text{Ca}(\text{H}_2\text{PO}_4)_2$ ) and water as shown in Eq. (3)<sup>25</sup>.



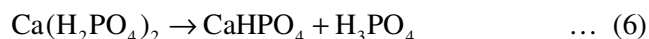
Or, the unhydrolysed CaO will react with phosphoric acid (Eq. 4).



The  $\text{Ca}(\text{H}_2\text{PO}_4)_2$  reacts readily with water to transform during heating to super-phosphate or monocalcium phosphate monohydrate ( $\text{Ca}(\text{H}_2\text{PO}_4)_2 \cdot \text{H}_2\text{O}$ ). This reacts with the remaining calcium hydroxide to yield brushite ( $\text{CaHPO}_4 \cdot 2\text{H}_2\text{O}$ ) (Eq. 5)<sup>25</sup>.



The above calcium dihydrogen phosphate may also decompose into monetite ( $\text{CaHPO}_4$ ) and phosphoric acid (Eq. 6).



$\text{Ca}(\text{H}_2\text{PO}_4)_2$  may react with ammonia to form  $\text{CaHPO}_4$  (Eq. 7).



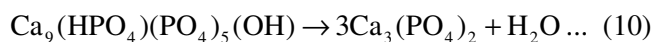
It is accordingly inferred that many overlapping reactions may occur since phosphoric acid and ammonium dihydrogen phosphate are produced at higher temperatures. Once the monetite or brushite is formed, it decomposes into calcium pyrophosphate ( $\text{Ca}_2\text{P}_2\text{O}_7$ ) and water at 700-900°C (Eqs 8 & 9)<sup>25</sup>.



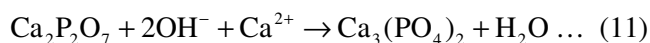
This is probably the reason for the additional weight losses observed in the samples **Ca-0** and **Ca-1** above 700°C. The calcium pyrophosphate may react

with CaO to form TCP ( $\text{Ca}_3(\text{PO}_4)_2$ ) at higher temperature<sup>25</sup>, as observed by the  $\text{P}_2\text{O}_7$  band at  $727\text{ cm}^{-1}$  in the IR spectra at calcination temperature above  $800^\circ\text{C}$ . However, the other intermediate phases are readily decomposed during heating into the subsequent phase at the given temperature and are not observed in the X-ray patterns.

In X-ray patterns of all of the samples calcined at  $700^\circ\text{C}$ , the observed peaks are broad, showing its low crystallinity. Such broad peaks can not merely be associated with less calcium in a sample because the samples **Ca-1** and **Ca-2** with excess calcium also show such broad peaks. It is suggested that the appearance of CDHA phase is not merely due to less calcium, but also due to incomplete transformation of HA. The TG-DTA curves suggest that the transformation reaction is still in progress at  $700^\circ\text{C}$  as the transformation is not complete above  $700^\circ\text{C}$ .  $\beta$ -TCP appears replacing the CDHA after the sample **Ca-0** is calcined at  $700^\circ\text{C}$ ; the  $\beta$ -TCP phase may come from decomposition of the CDHA as follows (Eq. 10)<sup>17</sup>:



In the sample **Ca-1**,  $\beta$ -TCP may be observed due to the condensation of  $\text{HPO}_4^{2-}$  upon heating into  $\text{P}_2\text{O}_7^{4-}$  and water as suggested elsewhere<sup>15,26</sup>. Simultaneously,  $\text{P}_2\text{O}_7^{4-}$  may react with O-H in the presence of ionic calcium to form  $\beta$ -TCP as described in following reaction (Eq. 11).



However for the sample **Ca-2**, another explanation for the very small  $\beta$ -TCP may be necessary because the  $\text{P}_2\text{O}_7^{4-}$  band is not observed in the IR spectra. A small amount of  $\text{NH}_4\text{H}_2\text{PO}_4$  may produce  $\text{P}_2\text{O}_5$  during heating<sup>27</sup> which reacts with CaO resulting in  $\text{Ca}_2\text{P}_2\text{O}_7$ , and  $\beta$ -TCP is then obtained as the following sequence of reactions shows (Eqs 12 & 13).



These results indicate that the remaining CaO in the solution will give a chance for  $\beta$ -TCP to appear along with HA. Two techniques have been used by many authors to get better purity of HA: the first<sup>14</sup>, pH of the solution was controlled during synthesis, the second<sup>28</sup>, the precipitation solution was to be washed several times to remove either phosphorus or

calcium compounds remaining in the solution before drying or aging. Unfortunately, the source of  $\text{Ca}_2\text{P}_2\text{O}_7$  is not only one, as described above. The monetite and brushite formed are also sources of calcium pyrophosphate ( $\text{Ca}_2\text{P}_2\text{O}_7$ ) and water at  $700$ - $900^\circ\text{C}$  and calcium hydroxide is the source of CaO. Thus, possibly  $\beta$ -TCP and CaO appear at the subsequent temperature.

## Conclusions

In the above studies, calcium phosphate materials with three different calcium contents, viz., stoichiometric CaO (**Ca-0**), 10 mole% excess CaO (**Ca-1**), and 20 mole% excess CaO (**Ca-2**) with 0.1 mole CaO as the base, have been successfully synthesized using CaO and  $\text{NH}_4\text{H}_2\text{PO}_4$  through low temperature hydrothermal process. The as prepared powders have been dried, followed by calcination at  $700$ - $1200^\circ\text{C}$  at  $100^\circ\text{C}$  interval. The difference in CaO content brought about difference in stability of the calcium phosphate phase over the different heating regimes. The samples **Ca-0**, **Ca-1** and **Ca-2** have been characterized as unstable, unstable and stable phase respectively. The appearance of  $\beta$ -TCP is due to calcium deficiency since its amount decreases with the increasing Ca content. Multiple reactions forming intermediates probably occur in the samples **Ca-0** and **Ca-1** causing the thermal instability of calcium phosphate phase. The X-ray analysis shows different lattice parameters in all the three samples. Even though all the samples have the  $c/a$  lattice ratio close to that of the standard, the sample **Ca-2** has the closest the atomic spacing  $d$ .

## Acknowledgement

One of the authors, (ASFA), would like to thank the Ministry of National Education, The Republic of Indonesia, for a scholarship, (No. 2865.33 & 2866.38/D4.4/2008).

## References

- 1 Dorozhkin S V, *J Mater Sci*, 43 (2008) 3028.
- 2 Sopyan I, Mel M, Ramesh S & Khalid K A, *Sci Technol Adv Mater*, 8 (2007) 116.
- 3 Kokoska M S, Friedman C D, Castellano R D & Costantino P D, *Arch Facial Plast Surg*, 6 (2004) 290.
- 4 Takano I & Ishi Y, *J Orthop Sci*, 2 (1997) 98.
- 5 Beloufa S, Chaair H, Loukili H, Digua J & Sallek B, *Mater Res*, 11 (2008) 93.
- 6 Dawson-Hughes B, Seligson F H & Hughes V A, *Am J Clin Nutr*, 44 (1986) 83.
- 7 Deb S, Giri J, Dasgupta S, Datta D & Bahadur D, *Bull Mater Sci*, 26 (2003) 655.

- 8 Gross K A, Jackson R, Cashion J D & Rodriguez-Lorenzo L M, *Eur Cells Mater Suppl*, 3 (2002) 114.
- 9 Fu Q, Zhou N, Huang W, Wang D, Zhang L & Li H, *J Biomed Mater Res*, 74A (2005) 156.
- 10 Aoki A, Ogaki M & Kano S, *Rep Inst Med Dent Eng*, 27 (1993) 39.
- 11 Ramesh S, Tan C Y, Bhaduri S B, Teng W D & Sopyan I, *J Mater Process Technol*, 206 (2008) 221.
- 12 Sopyan I, Singh R & Hamdi M, *Indian J Chem*, 47A (2008) 1626.
- 13 Murugan R & Ramakrishna S, *Am J Biochem Biotech*, 3 (2007) 118.
- 14 Bezzi G, Celotti G, Landi E, La Torretta T M G, Sopyan I & Tampieri A, *Mater Chem Phys*, 78 (2003) 816.
- 15 Markovic M, Fowler B O & Tung M S, *J Res Natl Inst Stand Technol*, 109 (2004) 553.
- 16 Ermrich M & Peters F, *Z Kristallogr Suppl*, 23 (2006) 523.
- 17 Gibson I R, Rehman I, Best S M & Bonfield W, *J Mater Sci Mater Med*, 11 (2000) 533.
- 18 Smith B, *Infrared Spectral Interpretation. A Systematic Approach*, (CRC Press, Boca Raton, London, New York, Washington D C) 1999, pp. 74
- 19 Neira I S, Guitan F, Taniguchi T, Watanabe T & Yoshimura M, *J Mater Sci*, 43 (2008) 2171.
- 20 Santos R V & Clayton R N, *Am Mineral*, 80 (1995) 336.
- 21 Nakamura S & Nakahira A, *J Ceram Soc Japan*, 116(1) (2008) 42.
- 22 Kreidler E R & Hummel F A, *Am Mineral*, 55 (1970) 170.
- 23 Landi E, Logroscino G, Proietti L, Tampieri A, Sandri M & Sprio S, *J Mater Sci Mater Med*, 19 (2008) 239.
- 24 Cheng Z H, Yasukawa A, Kandori K & Ishikawa T, *J Chem Soc Faraday Trans*, 94 (1998) 1501.
- 25 Forschungsvorhaben StSch 4386, *Industrielle Hinterlassenschaften der Rohphosphat-Verarbeitung* (Teil 3b, Andreas Reichelt, München) 2005, pp. 80, 82, 100, 115.
- 26 Ben-Nissan B, Chai C & Evans L, *Crystallographic and Spectroscopic Characterization and Morphology of Biogenic and Synthetic Apatites*, in *Encyclopedic Handbook of Biomaterials and Bioengineering, Part B: Applications, Vol. 1*, edited by D L Wise, D J Trantolo, D E Altobelli, M J Yaszemski, J D Gresser & E R Schwartz, (Marcel Dekker, New York) 1995, pp. 191-221.
- 27 Neiman R & Sarma A C, *J Dent Res*, 59 (1980) 1478.
- 28 Pramanik N, Biswas S K & Pramanik P, *Int J App Ceram Technol*, 5 (2008) 20.